CFD Letters 15, Issue 3 (2023) 112-122

CFD Letters

Journal homepage:
https://semarakilmu.com.my/journals/index.php/CFD_Letters/index
ISSN: 2180-1363

Boundary Layer Flow of Williamson Hybrid Ferrofluid over A Permeable Stretching Sheet with Thermal Radiation Effects

Wan Muhammad Hilmi Wan Rosli[1], Muhammad Khairul Anuar Mohamed[1,*], Norhafizah Md Sarif[1], Nurul Farahain Mohammad[2], Siti Khuzaimah Soid[3]

[1] Centre for Mathematical Sciences, College of Computing & Applied Sciences, University Malaysia Pahang, Lebuhraya Tun Razak 26300, Gambang, Kuantan, Pahang, Malaysia
[2] Department of Computational and Theoretical Sciences, Kulliyyah of Science, International Islamic University Malaysia, Bandar Indera Mahkota, 25200 Kuantan, Pahang, Malaysia
[3] Faculty of Computer and Mathematical Sciences, Universiti Teknologi MARA, 40450 UiTM Shah Alam, Selangor, Malaysia

ARTICLE INFO

Article history:
Received 6 September 2022
Received in revised form 10 October 2022
Accepted 9 November 2022
Available online 1 March 2023

Keywords:
Williamson hybrid ferrofluid; blood based; permeable stretching sheet; thermal radiation effects

ABSTRACT

This research investigated the convective boundary layer flow and heat transfer of Williamson hybrid ferrofluid over a permeable stretching sheet with thermal radiation effects. Human blood is employed as a based fluid while magnetite (Fe3O4) and copper (Cu) are taken as the hybrid ferroparticle. The study started with transforming the non-linear partial differential equation system that governed the model to a more convenience non-linear dimensionless ordinary differential equations using the similarity transformation. The transformed equations obtained then are solved numerically using the Runge-Kutta-Fehlberg (RKF45) method in Maple software. The characteristics and effects of stretching parameter, permeability parameter, thermal radiation parameter as well as the ferroparticle volume fraction in the Williamson hybrid ferrofluid towards the temperature profiles, velocity profiles as well as the Nusselt number and the skin friction coefficient are analysed and discussed. The result of this research for various pertinent parameter varies differently. It can be concluded that the increase in magnetic parameter, the Williamson parameter, the stretching parameter, and the permeability rate parameter increase the skin friction and reduced the velocity profile. Furthermore, the increase in stretching parameter, thermal radiation parameter and the permeability rate results to the increase in the Nusselt number.

1. Introduction

The illustration flow of pseudoplastic using model equation was proposed by Williamson [1]. It is a straightforward model which simulates the viscoelastic shear-thinning characteristics. Named as the Williamson fluid, it has a shear-thinning property where the rate of shear stress increases, the viscosity of fluid decreases which can be characterised as a fluid since the Newton's law of viscosity is disobeyed. Blood flow is one of the related examples to a Williamson fluid model. Nadeem *et al.,*

* *Corresponding author.*
E-mail address: mkhairulanuar@ump.edu.my (Muhammad Khairul Anuar Mohamed)

https://doi.org/10.37934/cfdl.15.3.112122

[2-6] have extended the Williamson model to fluid flow over stretching sheet, heated surface over a stretching sheet and peristaltic flow in asymmetrical channel.

Ferrofluid was introduced early in the days to help the astronaut to travel into space. NASA invented the fluid to overcome the zero gravity in space by mixed together with fuel (base fluid) so that the fuel can be injected into the combustion chamber using magnetic force [7]. Due to the fluid characteristic which can be moved with the presence of magnetic force, it attracts researcher to further study and extend the fluid capability including fluid interaction and heat transfer. The effect of frictional and joule heating on ferrofluid are studied by Reddy *et al.,* [8] which they include both Casson and Williamson models in constructing the basic flow equations in their study. Jiao *et al.,* [9] found in their studies found that to achieve the best result of heat transfer of ferrofluid the concentration of particle and external magnetic effect has to be controlled. Saeed *et al.,* [10] claimed velocity profile gradient decrease as ferrofluid and viscosity parameter increase. Ferrofluid is also used to create new smart fluid and solar application like [11-14].

There are many researcher who are interested in researching the fluid flow past a permeable stretching sheet and credit to Crane *et al.,* [15] who was the first to studied the boundary layer flow on stretching sheet. Investigating incompressible viscous fluid flow over a stretching plate, Crane discovered that the boundary layer for fluid velocity varied linearly using analytical solution. Kumaran *et al.,* [16] stated that the researchers extended Crane studies and obtained closed form solutions. They also concluded that the wall shear stress reduction is caused by the shear thinning property of the fluid. Jusoh *et al.,* [17] found that ferrofluid exert drag force when rotation parameter increases on the stretching surface. They also claimed increase gradient of velocity profile which translate that skin friction increase when suction, magnetic and nanoparticle volume fraction parameter increase. Jahan *et al.,* [18] found in their research of boundary layer flow of nanofluid on permeable stretching/shrinking sheet that increase of suction parameter is linear with heat transfer rate. Naramgari *et al.,* [19] also stated the same founding.

Other than conduction and convection, thermal radiation is another heat and energy transfer method, and it is the only heat transfer method that occurred without medium of transfer (vacuum). Surface temperature increases when received thermal radiation energy [20]. Since thermal radiation may affect the heat transfer on the surface, it is important to study the presence of it in this research. Recently, Kumar *et al.,* [21] analysed the impact of thermal radiation on nanofluid flow from an infinite vertical plate and establish that increasing thermal radiation parameter heightens both velocity and temperature profile. Abbas *et al.,* [22] and Megahed *et al.,* [23] both made the same claimed that skin friction and Nusselt number are in line with increasing radiation parameter. Other recent studies considering thermal radiation effects included the works by Mishra *et al.,* [24], Asghar *et al.,* [25], Daud *et al.,* [26] and Ismail *et al.,* [27].

In summary, studies on blood-based Williamson hybrid ferrofluid were not available to find. In this paper, the upgraded fluid called Williamson hybrid ferrofluid was investigated. A small amount of metal nanoparticles, copper (*Cu*) is blended with ferrofluid (Fe_3O_4) together in Williamson fluid (blood) is believed to provide better thermal properties compared to its conventional ferrofluid. With this research it will provide fast and cheap theoretical knowledge of the upgraded fluid characteristics of heat transfer and surface interaction using mathematical formulation and numerical solution.

2. Mathematical Formulation

Figure 1 below illustrates a steady two-dimensional Williamson hybrid ferrofluid flow on a permeable stretching sheet with ambient temperature. Assuming that $T = T_w$ is the wall temperature, u and v are the velocity components along the x and y axes, respectively. Next q_r

is the radiative heat flux and B_0 is the uniform magnetic field of strength that is assumed to be applied the positive y-directional normal to the flat plate.

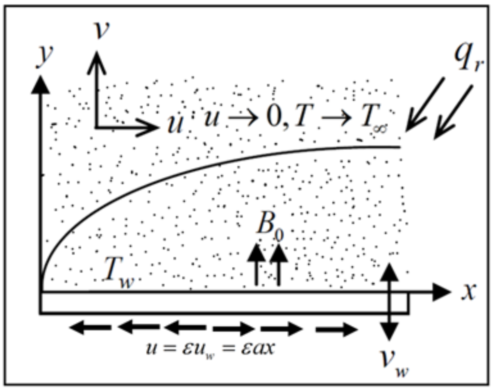

Fig. 1. Physical model and the coordinate system

The Navier-Stoke equations that can be formed are [20,28-30]:

$$\frac{\partial u}{\partial x} + \frac{\partial v}{\partial y} = 0, \tag{1}$$

$$u\frac{\partial u}{\partial x} + v\frac{\partial u}{\partial y} = \nu_{hnf}\frac{\partial^2 u}{\partial y^2} + \sqrt{2}\,\nu_{hnf}\,\Gamma\frac{\partial u}{\partial y}\frac{\partial^2 u}{\partial y^2} - \frac{\sigma B_o^2(x)}{\rho_{hnf}}u, \tag{2}$$

$$u\frac{\partial T}{\partial x} + v\frac{\partial T}{\partial y} = \frac{k_{hnf}}{\left(\rho C_p\right)_{hnf}}\frac{\partial^2 T}{\partial y^2} - \frac{1}{\left(\rho C_p\right)_{hnf}}\frac{\partial q_r}{\partial y}. \tag{3}$$

with boundary conditions:

$$\begin{aligned} &u = \varepsilon u_w = \varepsilon ax,\ v = v_w,\ T = T_w \text{ at } y = 0 \\ &u \to 0,\quad T \to T_\infty, \text{ as } y \to \infty \end{aligned} \tag{4}$$

ε is a stretching parameter and v_w is a plate permeability rate. Using the Rosseland approximation for radiation, the radiative heat flux is simplified as [31]:

$$q_r = -\frac{4\sigma^*}{3k^*}\frac{\partial T^4}{\partial y} \tag{5}$$

where σ^* and k^* are the Stefan-Boltzmann constant and the mean absorption coefficient, respectively. The hybrid ferrofluid kinematic viscosity, a dynamic viscosity, a density, and the electric conductivity are denoted as ν_{hnf}, μ_{hnf}, ρ_{hnf} and σ respectively. Furthermore, Γ, k_{hnf} and $(C_p)_{hnf}$ are the time constant, the thermal conductivity and the heat capacity of Williamson hybrid ferrofluid respectively. Other properties related to base fluid and the nanoparticles are denoted with subscript $_{bf}$ and $_{s1,s2}$ respectively. We assume that the temperature differences within the flow through the fluid such as that the term T^4 may be expressed as a linear function of temperature. Hence, expanding T^4 in a Taylor series about T_∞ and neglecting higher-order terms, we get:

$$T^4 \cong 4T_\infty^3 T - 3T_\infty^4 \tag{6}$$

In view of Eq. (5) and Eq. (6), Eq. (3) reduces to

$$u\frac{\partial T}{\partial x} + v\frac{\partial T}{\partial y} = \left(\frac{k_{hnf}}{\left(\rho C_p\right)_{hnf}} + \frac{16\sigma^* T_\infty^3}{3\left(\rho C_p\right)_{hnf} k^*}\right)\frac{\partial^2 T}{\partial y^2}. \tag{7}$$

The hybrid ferrofluid properties are given as [32,33]

$$\begin{gathered}
\nu_{hnf} = \frac{\mu_{hnf}}{\rho_{hnf}}, \quad \rho_{hnf} = (1-\phi_2)\left[(1-\phi_1)\rho_f + \phi_1\rho_{s1}\right] + \phi_2\rho_{s2}, \quad \mu_{hnf} = \frac{\mu_f}{(1-\phi_1)^{2.5}(1-\phi_2)^{2.5}}, \\
\left(\rho C_p\right)_{hnf} = (1-\phi_2)\left[(1-\phi_1)\left(\rho C_p\right)_f + \phi_1\left(\rho C_p\right)_{s1}\right] + \phi_2\left(\rho C_p\right)_{s2}, \\
\frac{k_{hnf}}{k_{bf}} = \frac{k_{s2} + 2k_{bf} - 2\phi_2(k_{bf} - k_{s2})}{k_{s2} + 2k_{bf} + \phi_2(k_{bf} - k_{s2})}, \quad \frac{k_{bf}}{k_f} = \frac{k_{s1} + 2k_f - 2\phi_1(k_f - k_{s1})}{k_{s1} + 2k_f + \phi_1(k_f - k_{s1})}
\end{gathered} \tag{8}$$

the similarity variable considered are as follows [29]:

$$\eta = \left(\frac{a}{\nu_f}\right)^{1/2} y, \ \psi = \left(a\nu_f\right)^{1/2} x f(\eta), \ \theta(\eta) = \frac{T - T_\infty}{T_w - T_\infty}, \tag{9}$$

where η, ψ and θ is a non-dimensional variable, dimensional stream function and temperature, respectively. The similarity variables Eq. (9) satisfy the continuity Eq. (1) by definition Eq. (10)

$$u = \frac{\partial \psi}{\partial y} \text{ and } v = -\frac{\partial \psi}{\partial x}. \tag{10}$$

Next, substitute the similarity variables Eq. (9) and Eq. (10) into governing Eq. (2) and Eq. (3) gives the following transformed ordinary differential equations:

$$\frac{1}{(1-\phi_1)^{2.5}(1-\phi_2)^{2.5}\left[(1-\phi_2) + \left[(1-\phi_1) + \phi_1(\rho_{s1}/\rho_f)\right] + \phi_2(\rho_{s2}/\rho_f)\right]} f''' + ff'' + \lambda f'' f''' - f'^2 - Mf' = 0, \tag{11}$$

$$\frac{k_{hnf}/k_f}{(1-\phi_2)\left[(1-\phi_1) + \phi_1(\rho C_p)_{s1}/(\rho C_p)_f\right] + \phi_2(\rho C_p)_{s2}/(\rho C_p)_f}\left(1 + \frac{4}{3}N_R\right)\theta'' + \Pr f\theta' = 0. \tag{12}$$

The boundary conditions Eq. (4) become

$$\begin{gathered}
f(0) = S, \ f'(0) = \varepsilon, \ \theta(0) = 1, \\
f'(\eta) \to 0, \ \theta(\eta) \to 0, \text{ as } y \to \infty.
\end{gathered} \tag{13}$$

By definition, $\Pr = \frac{\nu_f \left(\rho C_p\right)_f}{k_f}$ is a Prandtl number, $S = -\frac{v_w}{(a\nu_f)^{1/2}}$ is the permeability parameter at the plate surface, with *S*>0 and *S*<0 corresponds for suction and injection, respectively, $\lambda = x\Gamma\sqrt{\frac{2a^3}{\nu_{hnf}}}$ is the Williamson fluid parameter, $\varepsilon = \frac{a}{b}, (\varepsilon > 0)$ is a stretching parameter, $N_R = \frac{4\sigma^* T_\infty^3}{k^* k_{hnf}}$ is the thermal radiation parameter and $M = \frac{\sigma B_o^{\,2}(x)}{a\rho_{nf}}$ is the magnetic parameter. The physical quantities of interest are the skin friction coefficient C_f and the local Nusselt number Nu_x are given by:

$$C_f = \frac{\tau_w}{\rho_f u_w^2},\ Nu_x = \frac{xq_w}{k_f (T_w - T_\infty)}, \tag{14}$$

with the surface shear stress τ_w and the surface heat flux q_w are given by

$$\tau_w = \mu_{hnf}\left(\frac{\partial u}{\partial y} + \frac{\Gamma}{\sqrt{2}}\left(\frac{\partial u}{\partial y}\right)^2\right)_{\bar{y}=0},\ q_w = -k_{hnf}\left(\frac{\partial T}{\partial y}\right)_{\bar{y}=0} + q_r, \tag{15}$$

Using variables in Eq. (6) and Eq. (14) give

$$C_f \operatorname{Re}_x^{1/2} = \frac{1}{(1-\phi_1)^{2.5}(1-\phi_2)^{2.5}}\left(f''(0) + \frac{\lambda}{2} f''(0)^2\right) \text{ and } Nu_x \operatorname{Re}_x^{-1/2} = -\frac{k_{hnf}}{k_f}\left[1 + \frac{4}{3}N_R\right]\theta'(0) \tag{16}$$

3. Results

The non-linear ordinary differential Eq. (11) and Eq. (12) with boundary conditions Eq. (13) were solved using Runge-Kutta-Fehlberg (RKF45) method programmed in Maple software. RKF45 is a method of order 4 with an error estimator of order 5 based on the large class of Runge-Kutta method. It was developed by German mathematician, Erwin Fehlberg. RKF (45) method is used because of its stability, well-known accuracy, and it does not require initial value profile.

In this research, $\Pr$ is set to 21 due to consideration of blood as a based fluid. Following Devi *et al.,* [32], initially 0.1 vol. solid nanoparticle of $Fe_3O_4\,(\phi_1 = 0.1)$ is added into blood to form *Fe₃O₄*/blood ferrofluid. Next, the 0.06 solid nanoparticle of $Cu\,(\phi_2 = 0.06)$ is added into Fe_3O_4/blood ferrofluid to form the hybrid ferrofluid namely Fe_3O_4-*Cu*/blood hybrid ferrofluid. Table 1 shows the thermophysical properties of blood, magnetite (Fe_3O_4) and copper (Cu). To validate the numerical method accuracy, present result was compared with previous numerical result reported by Salleh *et al.,* [29] as shown in Table 2. The result of present research for $-\theta'(0)$ with previous result was in good agreement.

Table 1
Thermophysical properties of water, ferroparticles and copper particles [33]

Physical Properties	Blood	Magnetite (Fe_3O_4), ϕ_1	Copper (Cu), ϕ_2
ρ (kg/m^3)	1053	5180	8933
C_p (J/kg·K)	3594	670	385
k(W/m·K)	0.492	9.7	400

Table 2
Comparison values of $-\theta'(0)(CWT)$ with previously published result when $\phi_1 = \phi_2 = M = \lambda = \varepsilon = Nr = S = 0$

Pr	$-\theta'(0)$	
	Salleh *et al.,* [29]	Present Paper
0.72	0.46317	0.466972
1	0.58198	0.582663
3	1.16522	1.165164
10	2.30821	2.307950

The effects of thermal radiation parameter Nr as well as various nano particle volume fraction are illustrated in Figures 2 and 3. From Figure 2, it shows that the *Fe₃O₄-Cu*/blood hybrid ferrofluid ($\phi_1 = 0.1, \phi_2 = 0.06$) scored highest in $Nu_x \mathrm{Re}_x^{-1/2}$. Physically, *$Fe_3O_4$-Cu*/blood hybrid ferrofluid has better performance in heat transfer compared to blood-based viscous fluid ($\phi_1 = \phi_2 = 0$) and *Fe_3O_4*/blood ferrofluid ($\phi_1 = 0.1, \phi_2 = 0$). Its performance is almost similar with the concentrated *Fe_3O_4*/blood ferrofluid ($\phi_1 = 0.16, \phi_2 = 0$) as Nr increases. Even though it has the same performance of heat transfer as concentrated ferrofluid, Figure 3 shows that the *Fe_3O_4-Cu*/blood hybrid ferrofluid ($\phi_1 = 0.1, \phi_2 = 0.06$) has lower skin friction compared to *Fe_3O_4*/blood ferrofluid ($\phi_1 = 0.16, \phi_2 = 0$) but higher than blood-based viscous fluid and *Fe_3O_4*/blood ferrofluid ($\phi_1 = 0.1, \phi_2 = 0$). This is because higher concentration of ferrofluid exert drag to the surface. Besides that, it is found that the increase of Nr does not affect the skin friction of *Fe_3O_4*/blood ferrofluid ($\phi_1 = 0.1, \phi_2 = 0$), it produces constant $C_f \mathrm{Re}_x^{1/2}$ values throughout the parameter. This phenomenon is realistic where Nr has no relation with velocity term in Eq. (12). Noticed that the negative values stated in the Figure 3 refers to the opposing direction between fluid and the stretching sheet.

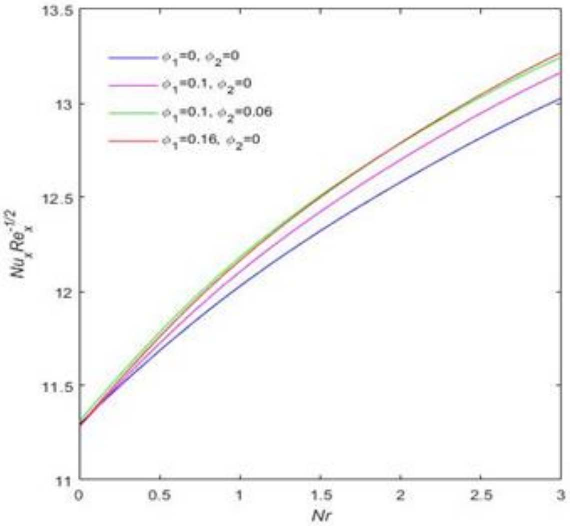

Fig. 2. Distribution of $Nu_x \mathrm{Re}_x^{-1/2}$ of different nano particle volume fractions for Nr when $\mathrm{Pr}=21,\ M=0.5,\ \lambda=0.1,\ \varepsilon=0.5,\ S=1$

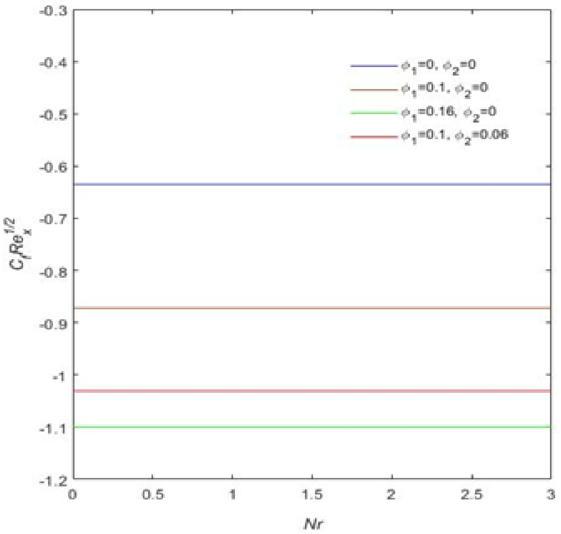

Fig. 3. Distribution of $C_f \mathrm{Re}_x^{1/2}$ of different nano particle volume fractions for Nr when $\mathrm{Pr}=21,\ M=0.5,\ \lambda=0.1,\ \varepsilon=0.5,\ S=1$

Table 3 shows the result of $Nu_x \mathrm{Re}_x^{-1/2}$ and $C_f \mathrm{Re}_x^{1/2}$ for various values of magnetic parameter M . Increasing strength of magnetic effects causes inclination of $C_f \mathrm{Re}_x^{1/2}$ values and reduction in $Nu_x \mathrm{Re}_x^{-1/2}$ values. Magnetic parameter induces Lorentz force which slow down the fluid velocity via ferroparticles, thus opposes the flow and increase the skin friction values.

Table 3
Results for various values of M with $Pr = 21, \lambda = 1,$ $\varepsilon = 0.5, Nr = 1, S = 0.5$

M	$Nu_x \mathrm{Re}_x^{-1/2}$	$C_f \mathrm{Re}_x^{1/2}$
0	12.2803016	-0.8688633
1	12.1087018	-1.2784927
2	11.9985094	-1.5645186
5	11.7891222	-2.1759994
10	11.5872789	-2.8826120

Next, Table 4 shows results for $Nu_x \mathrm{Re}_x^{-1/2}$ and $C_f \mathrm{Re}_x^{1/2}$ with various values of Williamson parameter. Both $Nu_x \mathrm{Re}_x^{-1/2}$ and $C_f \mathrm{Re}_x^{1/2}$ shows small changes when the Williamson parameter increases.

Table 4
Results for various values of λ with $Pr = 21, \mathrm{M} = 0.5, \varepsilon = 0.5, Nr = 1, S = 0.5$

λ	$Nu_x \mathrm{Re}_x^{-1/2}$	$C_f \mathrm{Re}_x^{1/2}$
0.1	12.1819220	-1.0990131
0.2	12.1709190	-1.1342526
0.3	12.1586059	-1.1759510
0.4	12.1446026	-1.2269258

Table 5 shows the effects of a stretching parameter ε on both $Nu_x \mathrm{Re}_x^{-1/2}$ and $C_f \mathrm{Re}_x^{1/2}$. As ε increases, it is observed that both $Nu_x \mathrm{Re}_x^{-1/2}$ and $C_f \mathrm{Re}_x^{1/2}$ increases. Physically, as ε increases, the stretching velocity increases, thus drag the fluid together with the plate. This situation raised the temperature gradient, physically known as the reduced Nusselt number.

Table 5
Results for various values of ε with $Pr = 21, \mathrm{M} = 0.5, \lambda = 0.1, Nr = 1, S = 0.5$

ε	$Nu_x \mathrm{Re}_x^{-1/2}$	$C_f \mathrm{Re}_x^{1/2}$
0.6	12.490567	-1.362532
0.8	13.059310	-1.923475
1	13.576097	-2.523478
1.2	14.051215	-3.155929
1.4	14.491423	-3.814647

Lastly, Table 6 shows the effects of a permeability rate parameter S on both $Nu_x \mathrm{Re}_x^{-1/2}$ and $C_f \mathrm{Re}_x^{1/2}$ values. Noted that (*S<0*) and (*S>0*) are the injection and suction parameters respectively. It can be concluded that increasing the *S* parameter results to the increase in both quantities. This result is in line with the claim from Jahan *et al.,* [18] and Naramgari *et al.,* [19]. Result for permeability injection rate (*S<0*) will be the opposite of permeability suction rate (*S>0*) where skin friction and

Nusselt number value are decreasing. Noticed that the large injection rate effect may promote to pure conduction heat transfer process ($Nu_x \mathrm{Re}_x^{-1/2} \simeq 0$).

Table 6
Results for various values of S with $Pr = 21, \mathrm{M} = 0.5, \varepsilon = 0.5, \lambda = 0.1, \mathrm{Nr} = 1$

S	$Nu_x \mathrm{Re}_x^{-1/2}$	$C_f \mathrm{Re}_x^{1/2}$
-0.8	0.000123	-0.542655
-0.6	0.015589	-0.601733
-0.4	0.332867	-0.669632
-0.2	1.611840	-0.747152
0	3.933716	-0.834844
0.5	12.181922	-1.099013
1	21.683097	-1.420965
1.2	25.607000	-1.562865
1.4	29.568223	-1.710816

4. Conclusions

The effects of the magnetic parameter, the Williamson parameter, the stretching parameter, the permeability rate parameter, and the thermal radiation parameter on the Nusselt number and the skin friction coefficient of blood-based Williamson hybrid ferrofluid is numerically studied. Below shows the summary of the results:

i. The hybrid ferrofluid has same performance of heat transfer with ferrofluid with the same volume of nanoparticle volume fraction, but it provided lower values of skin friction coefficient which physically gave less erosion on surface.
ii. Increasing all parameter resulted the increased in skin friction coefficient except for the thermal radiation parameter.
iii. Enhancing stretching parameter, permeability rate parameter and the thermal radiation parameter raised the Nusselt number while the magnetic parameter and the Williamson parameter developed oppositely.

Acknowledgement
Authors are grateful to acknowledge the Tabung Persidangan Dalam Negara UMP and the IIUM-UMP-UiTM Sustainable Research Collaboration Grant 2020 (SRCG) under grant No. IIUM/504/G/14/3/1/1/SRCG20-0004 (University reference RDU200712) for providing the financial support.

References
[1] Williamson, R. Vo. "The flow of pseudoplastic materials." *Industrial & Engineering Chemistry* 21, no. 11 (1929): 1108-1111. https://doi.org/10.1021/ie50239a035
[2] Nadeem, S., and Safia Akram. "Influence of inclined magnetic field on peristaltic flow of a Williamson fluid model in an inclined symmetric or asymmetric channel." *Mathematical and Computer Modelling* 52, no. 1-2 (2010): 107-119. https://doi.org/10.1016/j.mcm.2010.02.001
[3] Akbar, Noreen Sher, Tasawar Hayat, S. Nadeem, and S. Obaidat. "Peristaltic flow of a Williamson fluid in an inclined asymmetric channel with partial slip and heat transfer." *International Journal of Heat and Mass Transfer* 55, no. 7-8 (2012): 1855-1862. https://doi.org/10.1016/j.cnsns.2009.07.026

[4] Nadeem, S., and S. T. Hussain. "Heat transfer analysis of Williamson fluid over exponentially stretching surface." *Applied Mathematics and Mechanics* 35, no. 4 (2014): 489-502. https://doi.org/10.1007/s10483-014-1807-6
[5] Nadeem, Sohail, and Syed Tayyab Hussain Hussain. 2016. "Analysis of MHD Williamson Nano Fluid Flow over a Heated Surface." *Journal of Applied Fluid Mechanics* 9 (2): 729-739. https://doi.org/10.18869/acadpub.jafm.68.225.21487
[6] Nadeem, Sohail, and S. T. Hussain. "Analysis of MHD Williamson nano fluid flow over a heated surface." *Journal of Applied Fluid Mechanics* 9, no. 2 (2016): 729-739. https://doi.org/10.1590/s0104-66322013000300019
[7] Papell, S. S. "Low viscosity magnetic fluid obtained by the colloidal suspension of magnetic particles Patent." (1965).
[8] Reddy, J. V., V. Sugunamma, and N. Sandeep. "Combined effects of frictional and joule heating on MHD nonlinear radiative Casson and Williamson ferrofluid flows with temperature dependent viscosity." *International Journal of Applied and Computational Mathematics* 4, no. 6 (2018): 1-25. https://doi.org/10.1007/s40819-018-0572-0
[9] Jiao, Feng, Qian Li, Yanying Jiao, and Yongqing He. "Heat transfer of ferrofluids with magnetoviscous effects." *Journal of Molecular Liquids* 328 (2021): 115404. https://doi.org/10.1016/j.molliq.2021.115404
[10] Saeed, Munazza, Bilal Ahmad, and Qazi Mahmood ul Hassan. "Variable thermal effects of viscosity and radiation of ferrofluid submerged in porous medium." *Ain Shams Engineering Journal* 13, no. 4 (2022): 101653. https://doi.org/10.1016/j.asej.2021.101653
[11] Chen, Jingge, Quanliang Cao, and Xiaotao Han. "Smart water-based ferrofluid with stable state transition property: Preparation and its application in anionic dye removal." *Journal of Cleaner Production* 287 (2021): 125003. https://doi.org/10.1016/j.jclepro.2020.125003
[12] Dahmani, A., J. Muñoz-Cámara, S. Laouedj, and J. P. Solano. "Heat transfer enhancement of ferrofluid flow in a solar absorber tube under non-uniform magnetic field created by a periodic current-carrying wire." *Sustainable Energy Technologies and Assessments* 52 (2022): 101996. https://doi.org/10.1016/j.seta.2022.101996
[13] Sahoo, R., P. Ussa-Aldana, D. Lancon, F. Rondelez, J. R. Morillas, R. Hidalgo-Alvarez, and J. de Vicente. "Design of smart lubricants using the inverse ferrofluid approach." *Tribology International* 166 (2022): 107346. https://doi.org/10.1016/j.triboint.2021.107346
[14] Shojaeizadeh, Ehsan, Farzad Veysi, Kourosh Zareinia, and Amir Mohammad Mansouri. "Thermal efficiency of a ferrofluid-based flat-plate solar collector under the effect of non-uniform magnetic field." *Applied Thermal Engineering* 201 (2022): 117726. https://doi.org/10.1016/j.applthermaleng.2021.117726
[15] Crane, Lawrence J. "Flow past a stretching plate." *Zeitschrift für angewandte Mathematik und Physik ZAMP* 21, no. 4 (1970): 645-647. https://doi.org/10.1007/bf01587695
[16] Kumaran, V., A. K. Banerjee, A. Vanav Kumar, and K. Vajravelu. "MHD flow past a stretching permeable sheet." *Applied mathematics and computation* 210, no. 1 (2009): 26-32. https://doi.org/10.1016/j.amc.2008.10.025
[17] Jusoh, Rahimah, Roslinda Nazar, and Ioan Pop. "Magnetohydrodynamic rotating flow and heat transfer of ferrofluid due to an exponentially permeable stretching/shrinking sheet." *Journal of Magnetism and Magnetic Materials* 465 (2018): 365-374. https://doi.org/10.1016/j.jmmm.2018.06.020
[18] Jahan, Shah, Hamzah Sakidin, Roslinda Nazar, and Ioan Pop. "Analysis of heat transfer in nanofluid past a convectively heated permeable stretching/shrinking sheet with regression and stability analyses." *Results in Physics* 10 (2018): 395-405. https://doi.org/10.1016/j.rinp.2018.06.021
[19] Naramgari, Sandeep, and C. Sulochana. "MHD flow over a permeable stretching/shrinking sheet of a nanofluid with suction/injection." *Alexandria Engineering Journal* 55, no. 2 (2016): 819-827. https://doi.org/10.1016/j.aej.2016.02.001
[20] Mohamed, Muhammad Khairul Anuar, Farah Nadia Abas, and Mohd Zuki Salleh. "MHD boundary layer flow over a permeable flat plate in a ferrofluid with thermal radiation effect." In *Journal of Physics: Conference Series*, vol. 1366, no. 1, p. 012014. IOP Publishing, 2019. https://doi.org/10.1088/1742-6596/1366/1/012014
[21] Kumar, M. Anil, Y. Dharmendar Reddy, V. Srinivasa Rao, and B. Shankar Goud. "Thermal radiation impact on MHD heat transfer natural convective nano fluid flow over an impulsively started vertical plate." *Case studies in thermal engineering* 24 (2021): 100826. https://doi.org/10.1016/j.csite.2020.100826
[22] Abbas, Amir, Iqra Ijaz, Muhammad Ashraf, and Hafeez Ahmad. "Combined effects of variable density and thermal radiation on MHD Sakiadis flow." *Case Studies in Thermal Engineering* 28 (2021): 101640. https://doi.org/10.1016/j.csite.2021.101640
[23] Megahed, Ahmed M., M. Gnaneswara Reddy, and W. Abbas. "Modeling of MHD fluid flow over an unsteady stretching sheet with thermal radiation, variable fluid properties and heat flux." *Mathematics and Computers in Simulation* 185 (2021): 583-593. https://doi.org/10.1016/j.matcom.2021.01.011

[24] Mishra, Jayaprakash, and Tumbanath Samantara. "Study of Unsteady Two Phase Flow over An Inclined Permeable Stretching Sheet with Effects of Electrification and Radiation." *Journal of Advanced Research in Fluid Mechanics and Thermal Sciences* 97, no. 2 (2022): 26-38. https://doi.org/10.37934/arfmts.97.2.2638

[25] Asghar, Adnan, Teh Yuan Ying, and Khairy Zaimi. "Two-Dimensional Magnetized Mixed Convection Hybrid Nanofluid Over a Vertical Exponentially Shrinking Sheet by Thermal Radiation, Joule Heating, Velocity and Thermal Slip Conditions." *Journal of Advanced Research in Fluid Mechanics and Thermal Sciences* 95, no. 2 (2022): 159-179. https://doi.org/10.37934/arfmts.95.2.159179

[26] Daud, Marjan Mohd, Lim Yeou Jiann, Rahimah Mahat, and Sharidan Shafie. "Application of Caputo Fractional Derivatives to the Convective Flow of Casson Fluids in a Microchannel with Thermal Radiation." *Journal of Advanced Research in Fluid Mechanics and Thermal Sciences* 93, no. 1 (2022): 50-63. https://doi.org/10.37934/arfmts.93.1.5063

[27] Ismail, Nurul Syuhada, Yong Faezah Rahim, Norihan Md Arifin, Roslinda Nazar, and Norfifah Bachok. "Stability Analysis of The Stagnation-Point Flow and Heat Transfer Over a Shrinking Sheet in Nanofluid in The Presence of MHD and Thermal Radiation." *Journal of Advanced Research in Fluid Mechanics and Thermal Sciences* 91, no. 2 (2022): 96-105. https://doi.org/10.37934/arfmts.91.2.96105

[28] Yasin, Siti Hanani Mat, Muhammad Khairul Anuar Mohamed, Zulkhibri Ismail, Basuki Widodo, and Mohd Zuki Salleh. "Numerical solution on MHD stagnation point flow in ferrofluid with Newtonian heating and thermal radiation effect." *Journal of Advanced Research in Fluid Mechanics and Thermal Sciences* 57, no. 1 (2019): 12-22.

[29] Salleh, M. Z., R. Nazar, and I. Pop. 2010. "Boundary layer flow and heat transfer over a stretching sheet with Newtonian heating." *Journal of the Taiwan Institute of Chemical Engineers* 41 (6): 651-655. https://doi.org/10.1016/j.jtice.2010.01.013

[30] Salleh, Mohd Zuki, Roslinda Nazar, and I. Pop. "Boundary layer flow and heat transfer over a stretching sheet with Newtonian heating." *Journal of the Taiwan Institute of Chemical Engineers* 41, no. 6 (2010): 651-655.. https://doi.org/10.1088/1742-6596/1366/1/012011

[31] Z Zheng, Liancun, Chaoli Zhang, Xinxin Zhang, and Junhong Zhang. "Flow and radiation heat transfer of a nanofluid over a stretching sheet with velocity slip and temperature jump in porous medium." *Journal of the Franklin Institute* 350, no. 5 (2013): 990-1007. https://doi.org/10.1016/j.jfranklin.2013.01.022

[32] Devi, Suriya Uma, and SP Anjali Devi. "Heat transfer enhancement of cu− $ al_ {2} o_ {3} $/water hybrid nanofluid flow over a stretching sheet." *Journal of the Nigerian Mathematical Society* 36, no. 2 (2017): 419-433. https://ojs.ictp.it/jnms/index.php/jnms/article/view/147

[33] Yasin, Siti Hanani Mat, Muhammad Khairul Anuar Mohamed, Zulkhibri Ismail, and Mohd Zuki Salleh. "Magnetohydrodynamic Effects in Mixed Convection of Ferrofluid Flow at Lower Stagnation Point on Horizontal Circular Cylinder." *Journal of Advanced Research in Fluid Mechanics and Thermal Sciences* 86, no. 1 (2021): 52-63. https://doi.org/10.37934/arfmts.86.1.5263